Molten Ga as a Solvent for Exploratory Synthesis. Preparation, Structure, and Properties of Two Ternary Silicides $MNiSi_3$ (M = Sm, Y)

X. Z. Chen,[†] P. Larson,[‡] S. Sportouch,[†] P. Brazis,[§] S. D. Mahanti,[‡] C. R. Kannewurf,[§] and M. G. Kanatzidis*,[†]

Department of Chemistry and Center for Fundamental Materials Research, Department of Physics and Astronomy and Center for Fundamental Materials Research, Michigan State University, East Lansing, Michigan 48824-1322, and Department of Electrical and Computer Engineering, Northwestern University, Evanston, Illinois 60208-3118

Received June 23, 1998. Revised Manuscript Received October 23, 1998

Two ternary silicides, $MNiSi_3$ (M = Sm, Y), have been synthesized from Sm, Ni, and Si in molten Ga at 850 °C in sealed silica tubes. Both compounds form black shiny crystals and are stable even in aqua regia. The structures, determined by single-crystal X-ray diffraction, are orthorhombic, *Cmmm* (No. 65) with $Z = 4$, and have lattice parameters $a = 3.965(2)$ Å, $b = 21.144(2)$ Å, $c = 4.007(1)$ Å for M = Sm and $a = 3.930(2)$ Å, $b = 21.021(2)$ Å, $c = 3.960(1)$ Å for M = Y, respectively. Refinement based on F_o^2 yielded $R_1 = 0.0319$ and $wR_2 = 0.0712$ [$I > 2\ \sigma(I)$] for M = Sm and $R_1 = 0.0267$ and $wR_2 = 0.0688$ [$I > 2\sigma(I)$] for M = Y. The compounds adopt the $SmNiGe_3$ structure type with zigzag Si chains and Si dimers and exhibit metallic p-type electrical conductivity. Variable temperature magnetic susceptibility data suggest that Sm is 3+ and Ni has no magnetic moment. $SmNiSi_3$ has an antiferromagnetic transition at 12 K and follows the modified Curie−Weiss law above 12 K. Band structure calculations using density functional theory, generalized gradient approximation, full potential LAPW method, and also extended Hückel tight binding theory show that the materials are metallic and suggest that Ni is either neutral or in a reduced oxidation state. Additional insight into the bonding was obtained by extended Hückel calculations carried out on the $[NiSi_3]^{3-}$ framework under the assumption that Y is mostly 3+. These results suggest that the Si zigzag chain contains single bonds with a partial double bond character.

Introduction

Metal silicides are both scientifically and technologically important and have been extensively studied during the past several decades. Because of their hardness, chemical stability, and high melting point, silicides are well-known as high-temperature structural materials,[1] components in high-temperature furnaces,[2] and high-temperature coatings.[3] Transition metal silicides are also highly valued as electrical and magnetic materials; some are even superconductors.[4] Several new potential applications have been explored recently, such as thermoelectric energy conversion[5] and as compatible electrode materials in electronics applications.[6] Several reviews and research papers are available regarding the preparation, properties, crystal chemistry,[7] thermodynamics,[8] applications in silicon technology,[9] and materials aspects of silicides for advanced technologies.[10] Silicides are usually synthesized by direct reaction of the elements heated in a vacuum or in an inert atmosphere. The reaction temperatures are usually over 1200 °C and it is necessary to use an arc-welder or induction furnace. Although single crystals sometimes can be obtained by annealing or quenching the product, only powder samples are obtained in most situations using these traditional methods. This often makes crystal structure determination more difficult and could limit proper characterization. Some other preparative methods for silicides are also known, such as electrochemical synthesis[11] and chemical vapor-deposition,[12] but these methods are not routinely used.

* To whom correspondence should be addressed.
[†] Department of Chemistry and Center for Fundamental Materials Research, Michigan State University.
[‡] Department of Physics and Astronomy and Center for Fundamental Materials Research, Michigan State University.
[§] Northwestern University.

(1) Shah, D. M.; Berczik, D.; Anton, D. L.; Hecht, R. *Mater. Sci. Eng. A* **1992**, *155*, 45−57.
(2) Fitzer, E. In *Plansee Proceedings 1955*; Benesovsky, F., Ed.; Pergamon: London, 1956; Chapter 7.
(3) Meier, G. H. In *High-Temperature Ordered Intermetallic Alloys II*; Stoloff, N. S., Koch, C., Liu, C. T., Izumi, O., Eds.; Materials Research Society Symposium Proceedings 81; Materials Research Society: Pittsburgh, 1987; p 443.
(4) King, R. B. *Inorg. Chem*. **1990**, *29*, 2164−2170, and references therein.
(5) *CRC Thermoelectric Handbook;* CRC: Boca Raton, FL, and references therein.
(6) (a) Maex, K. *Mater. Sci. Eng. R* **1993**, *11*, 53−153. (b) Murarka, S. P. *Silicides for VLSi Application*; Academic Press: New York, 1983, and references therein.
(7) Aronsson, B.; Lundström, T.; Rundqvist, S. *Borides, Silicides and Phosphides*; Methuen & Co. Ltd.: London, 1965.
(8) (a) Schlesinger, M. E. *Chem. Rev*. **1990**, *90*, 607−628. (b) Chart, T. G. *A Critical Assessment of Thermochemical Data for Transition Metal-Silicon Systems*; NPL report on Chemistry 18; National Physical Laboratory: Teddington, U.K., 1972.
(9) Reader, A. H.; Vanommen, A. H.; Weijs, P. J. W.; Wolters, R. A. M.; Oostra, D. J. *Rep. Prog. Phys.* **1993**, *56* (11), 1397−1467.
(10) Maex, K. *Appl. Surf. Sci.* **1991**, *53*, 328−337.

10.1021/cm980447v CCC: $18.00
Published on Web 12/24/1998

Recently we reported that molten Al flux is an excellent medium for synthesizing Al-containing multinary silicides.[13] In this paper, we introduce Ga metal flux for the synthesis of silicides below 1000 °C. This method is good for both binary and multinary silicide synthesis. Here we report the structure and properties of the two ternary silicides $MNiSi_3$ (M = Sm, Y) synthesized in Ga flux. The significance of this work is the use of Ga metal flux to obtain single-crystal silicides with no Ga incorporation in the structure. The magnetic properties of $MNiSi_3$ type compounds (M = Gd−Lu, Y)[14] have been discussed previously, but no crystal structures were reported. $ScNiSi_3$[15a] and $YNiSi_3$[15b] were briefly described earlier, albeit, we believe in the incorrect space group, *Amm*2. After examining the reported structure of $ScNiSi_3$, we recognized that it is actually isostructural to the compounds described here and therefore the correct space group should be *Cmmm* (No. 65).

Experimental Section

Synthesis. In a N_2-filled drybox, Sm or Y, Ni, Si, and Ga were roughly mixed in a vial in several different molar ratios and transferred into an alumina or graphite container which was flame sealed in a quartz tube under high vacuum. The sample was first heated to 1000 °C for 4 h, then cooled to 850 °C in 5 h and kept at 850 °C for 4 days, and finally cooled to 150 °C in 4 days. The product was first examined on a warmed Al metal plate, which was used to keep Ga metal liquid, and a couple of black crystals were selected from the liquid by using a needle under a microscope. Then DMF/I_2 or HCl(aq) solution was used to remove the Ga flux. Because of its very low melting point, the excess Ga flux can also be separated from the product by filtering it through a warmed glass frit. Black shiny single crystals of the title compounds were thus obtained.

EDS Analysis. Quantitative microprobe analysis of the compound was performed with a JEOL JSM-35C Scanning electron microscope (SEM) equipped with a Tracor Northern energy dispersive spectroscopy (EDS) detector. Data were acquired using an accelerating voltage of 20 kV and 100 s accumulation time.[16]

X-ray Crystallography. Single-crystal X-ray diffraction data were collected at room temperature by using a Rigaku AFC6S four-circle diffractometer with Mo Kα (λ = 0.71073 Å, graphite monochromated) radiation. A full reciprocal lattice sphere of data was obtained from both compounds. An empirical absorption correction, based upon a PSI-scan, was applied to the data. The structures were solved by direct methods (SHELXS86[17]) with the TEXSAN[18] crystallographic software package. The structures were refined with the SHELXTL[19] package of programs. The crystallographic data are listed in Table 1, and atomic positions and *U* values are shown in Table 2, respectively.

Table 1. Crystallographic Data for $MNiSi_3$ (M = Sm, Y)

formula weight	293.33	231.89
crystal size, mm	0.12 × 0.04 × 0.15	0.08 × 0.04 × 0.12
a (Å)	3.965(2)	3.930(2)
b (Å)	21.144(2)	21.021(2)
c (Å)	4.007(1)	3.960(1)
V (Å^3)	335.9(2)	327.1(2)
Z	4	4
space group	*Cmmm* (No. 65)	*Cmmm* (No. 65)
d_{calc}(g cm^{-3})	5.800	4.709
$2\theta_{max}$ range (deg)	60	60
radiation	Mo Kα (λ = 0.71069 Å)	Mo Kα (λ = 0.71069 Å)
μ (mm^{-1})	23.694	24.215
index ranges	$-5 \le h \le 5$ $-29 \le k \le 29$ $-5 \le l \le 5$	$-5 \le h \le 5$ $-29 \le k \le 29$ $-5 \le l \le 5$
reflns collected	1958	1910
unique refls	321 [*R*(int) = 0.0365]	314 [*R*(int) = 0.0311]
R indices ($I > 2\sigma$)	$R_1 = 0.032$ $wR_2 = 0.071$	$R_1 = 0.027$ $wR_2 = 0.069$
R indices (all data)	$R_1 = 0.034$ $wR_2 = 0.117$	$R_1 = 0.032$ $wR_2 = 0.109$
max. peak and hole	3.256 and −3.046 e$^-$/Å^3	1.339 and −1.186 e$^-$/Å^3

[a] $R_1 = \sum||F_o| - |F_c||/\sum|F_o|$; $wR_2 = [\sum(|F_o^2 - F_c^2|)^2/\sum(wF_o^2)^2]^{1/2}$.

Table 2. Atomic Positions and Equivalent Isotropic Displacement Parameters (Å^2) for $MNiSi_3$ (M = Sm, Y)[a]

atom	position	*x*	*y*	*z*	*U*(eq)[b]
Sm(1)	4j	0	0.3318(1)	0.5	4(1)
Y(1)		0	0.3314(1)	0.5	6(1)
Ni(1)	4i	0	0.1091(1)	0	5(1)
		0	0.1102(1)	0	6(1)
Si(1)	4j	0	0.0554(1)	0.5	7(1)
		0	0.0558(1)	0.5	7(1)
Si(2)	4i	0	0.2176(1)	0	5(1)
		0	0.2178(1)	0	6(1)
Si(3)	4i	0	0.4445(1)	0	7(1)
		0	0.4441(1)	0	7(1)

[a] Each first line is for M=Sm; each second line is for M=Y. [b] *U*(eq) is defined as one-third of the trace of the orthogonalized U_{ij} tensor.

Magnetic susceptibilities were measured with a Quantum Design SQUID magnetometer at temperatures between 2 and 300 K. Selected single crystals were ground to powder for the measurements. Magnetic susceptibility as a function of field strength (at a constant temperature of 300 K) was first investigated to determine if the samples experienced saturation of their magnetic signal. For all compounds, magnetization increased linearly with increasing field strength over the range investigated (100−55 000 G). The subsequent temperature-dependent studies were performed at low to moderate field strengths (300−5000 G).

DC electric conductivity and thermopower measurements were made on single crystals. Conductivity measurements were performed with the usual four-probe technique.[20] Thermopower measurements were made by using a slow ac technique.[21]

(11) Shapoval, V. I.; Malyshev, V. V.; Novoselova, I. A.; Kushkhov, K. B. *Russ. J. Appl. Chem.* **1994**, *67*, 828−833.
(12) Madar, R.; Thomas, N.; Bernard, C. *Mater. Sci. Eng. B* **1993**, *17*, 118−125, and references therein.
(13) Chen, X. Z.; Sportouch, S.; Sieve, B.; Cowen, J.; Kannewurf, C. R.; Brazis, P.; Kanatzidis, M. G. Accepted.
(14) *CRC Handbook of Crystal Structures and Magnetic Properties of Rare Earth Intermetallics*, CRC: Boca Raton, 1994; pp 110, and refs 3 and 4 therein.
(15) (a) Kotur, B. Ya.; Bodak, O. I.; Mys'kiv, M. G.; Gladyshevskii, E. I. *Sov. Phys. Crystallogr.* **1977**, *22*(2), 151−153. (b) Yarovets V. I. *Vestn. L'vov. Un-ta. Ser. Khim.* **1977**, 30−34.
(16) The analyses were made on several different crystals obtained from different reaction batches, and the results were quite consistent with an average formula of $MNiSi_2$ (M = Sm, Y). It was found that the fraction of Si obtained from EDS is always lower than that obtained from X-ray refinement and a correction factor must be applied.
(17) Sheldrick, G. M. In *Crystallographic Computing 3*; Sheldrick, G. M., Kruger, C. C., Doddard, R., Eds.; Oxford University Press: Oxford, UK, 1985; pp 175−189.
(18) "TEXSAN"−TEXRAY Structure Analysis Package", Molecular Structure Corporation, The Woodlands, TX, 1992.
(19) Sheldrick, G. M. 1995, SHELXL. Structure Determination Programs, Version 5.0. Siemens Analytical X-ray Instruments Inc., Madison, WI.
(20) (a) McCarthy, T. J.; Ngeyi, S.-P.; Liao, J.-H.; DeGroot, D.; Hogan, T.; Kannewurf, C. R.; Kanatzidis, M. G., *Chem. Mater.* **1993,** *5*, 331−340 (b) Lyding, J. W.; Marcy, H. O.; Marks, T. J.; Kannewurf, C. R. *IEEE Trans. 1nstrum. Meas.* **1988**, *37*, 76−80
(21) Chaikin, P. I.; Kwak, J. F. *Rev. Sci. Instrum.* **1975**, *46*, 218−220.

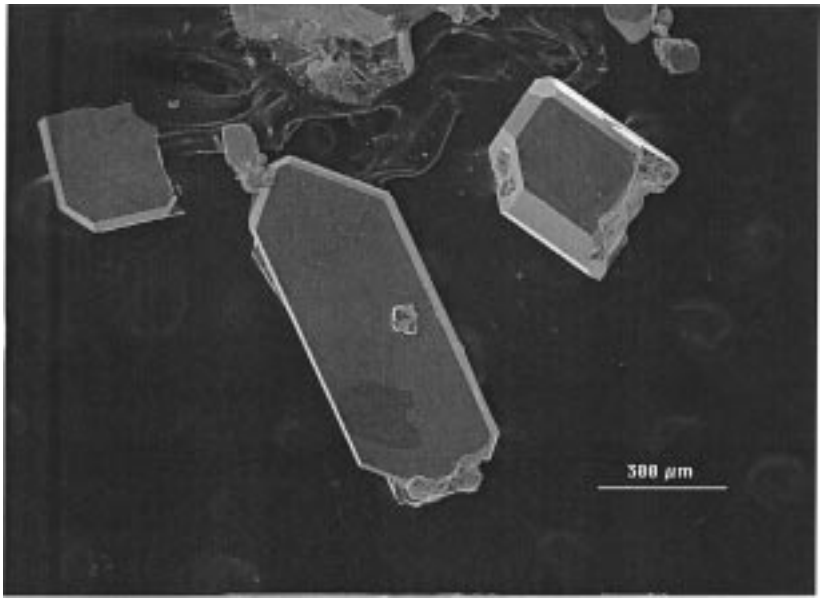

Figure 1. Crystals of $YNiSi_3$ grown from Ga flux.

Results and Discussion

Synthesis. Ga is unique as an element because it has the longest temperature range in the liquid phase. It melts at 29.78 °C and does not boil until 2403 °C. Thus, it potentially can be used as a solvent for a variety of reaction systems with different temperature requirements. For silicide synthesis, Ga seems particularly good because it solubilizes Si at elevated temperature. This is supported by the fact that when excess Si is used in the reaction, large Si crystals are frequently found among the reaction products. The Ga/Si phase diagram shows an eutectic point of 29.77 °C at only about 0.006 mol % of Si.[22] In addition, molten Ga does not react with Si, a very important property which makes Ga metal suitable for the synthesis and crystal growth of silicides. With rapid Si diffusion in the system comes increased reactivity with the other metals, which initiates phase formation. On the basis of the reaction temperature and time, both kinetic or thermodynamic phases can be formed. All elements are to a certain extent soluble in Ga, and in this sense the latter is not different from any conventional solvent. In the case described in this report, Sm or Y, Ni, and Si react in the Ga flux. EDS analyses on several different crystals show no detectable elemental Ga in the compounds.

Structure Description. Both compounds $MNiSi_3$ (M = Sm, Y) form black shiny crystals which are stable in concentrated HCl, HNO_3, and aqua regia. The crystals are well formed and faceted and achieve milimeter size dimensions; see Figure 1. In the absence of Ga as a solvent, arc-welding temperatures are necessary to even form a microcrystalline version of the compound.

The three-dimensional structure of $MNiSi_3$ (M = Sm, Y) is shown in Figure 2. The compounds crystallize in the $SmNiGe_3$ structure type[23] in space group *Cmmm*. The structure of $MNiSi_3$ (M = Sm, Y) contains pseudo-

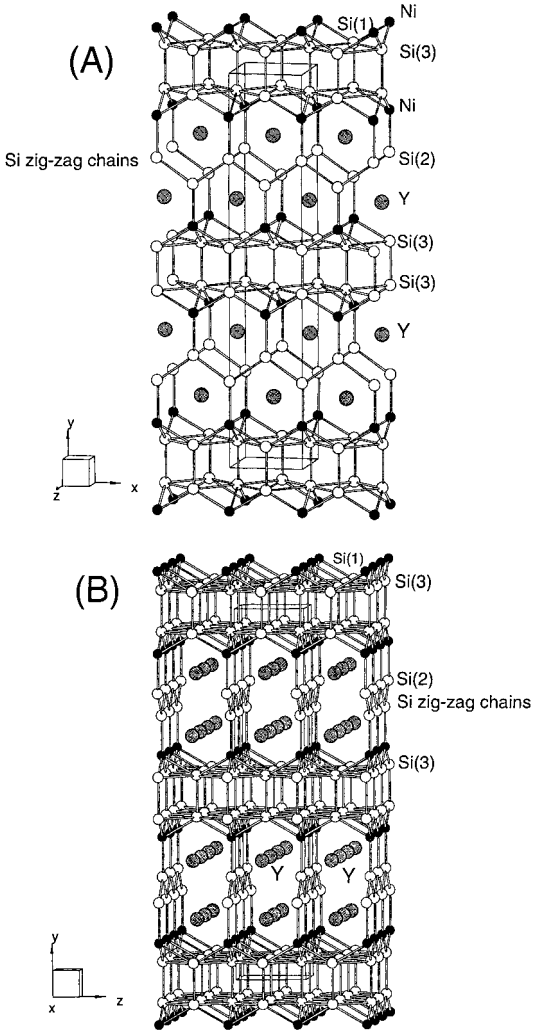

Figure 2. Two views of the three-dimensional structure of $YNiSi_3$: (A) view down the [001] direction and (B) view down the [100] direction.

hexagonal nets formed by Si and Ni atoms in the *ab*-plane; see Figure 2. There are two different types of polysilicide fragments, Si dimers [Si(1)−S(1) and Si(3)−

(22) *Binary Alloy Phase Diagrams;* Massalski, T. B., Ed.; American Society for Metals: Metals Park, Ohio, 1986.
(23) Bodak, O. I.; Pecharskii V. K.; Mruz, O. Ya.; Zavodnik, V. E.; Vilvitsaya, G. M.; Salamanko P. S. *Dopo.i Akad. Nauk Ukrains'Koi RSR, Seriya B* **1985**, *2*, 37.

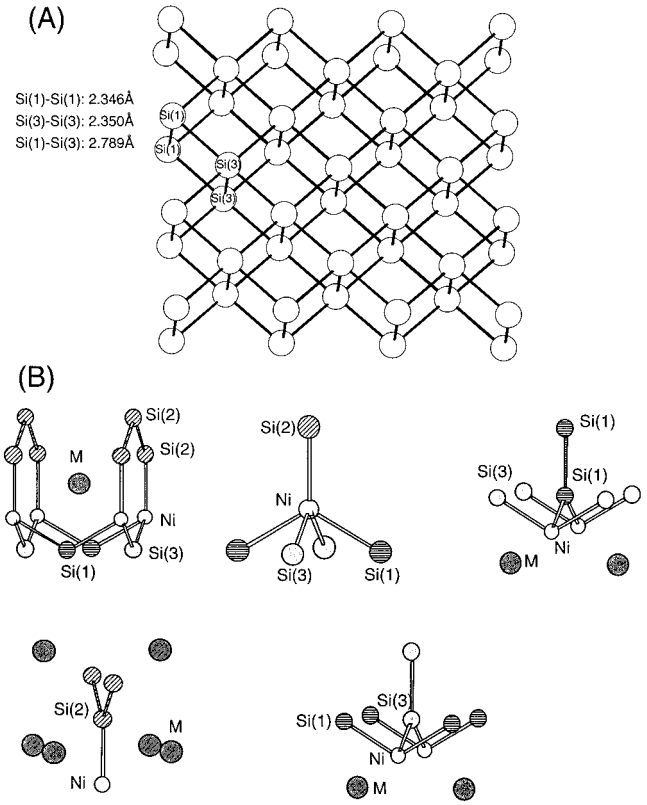

Figure 3. The local coordination environments for different atoms. In part B the Si(1)−Si(3) bond is not drawn for clarity.

Si(3)] and infinite zigzag Si(2) chains. The two different polysilicide fragments are segregated in two areas. The Si dimers are collinear with the *b*-axis direction and are arranged side by side in a rectangular array which extends over the *ac*-plane (Figure 2). The Si−Si distance in these dimers is ∼2.34 Å (average for both compounds) and is the same as that in elemental Si. It is interesting to note that the Si−Si distances between dimers are very short (∼2.8 Å) compared to the van der Waals distance of 3.8 Å, and they are most probably bonding (see below). This then gives rise to a fully bonded bilayer of rectangularly packed Si atoms sandwiched between two layers of Ni atoms; see Figure 3. The infinite zigzag Si chains are parallel to the *a*-axis with the plane of the zigzag chain being parallel to the crystallographic *ab*-plane. Within the zigzag chains the Si−Si distance is 2.409 and 2.385 Å for the Sm and Y compounds, respectively, and the Si−Si−Si angle, for both, is 110.8°. The Si chains and Si dimers are connected via Ni atoms, which are found in a slightly distorted square pyramidal coordination geometry (Figure 3B). This produces a three-dimensional tunnel framework with Sm (or Y) atoms filling the tunnels (Figure 2). Selected bond distances and angles are listed in Table 3.

The Sm (or Y) coordination environment is shown in Figure 3B and it is essentially a "pocket" made of two parallel Ni_2Si_4 hexagonal rings linked by bridging Si atoms via Ni−Si−Si bonds. In $SmNiSi_2$,[24] the Sm atom has the same coordination environment as in $SmNiSi_3$, and one of its two independent Si atoms forms one-dimensional zigzag chains as well. There are no Si−Si dimers, however, in $SmNiSi_2$. It is interesting to note that Si zigzag chains also exist in $Y_3(Ni_{0.5}Si_{0.5})Si_2$, with Si−Si of 2.42 Å and Si−Si−Si angles of 109.83°.

(24) Gil, A.; Szytula, A.; Tomkowicz, Z.; Wojciechowski, K. *J. Magn. Magn. Mater.* **1994**, *129*, 271−278 and refs 7 and 8 therein.

Table 3. Selected Bond Distances (Å) and Angles (deg) for $MNiSi_3$ (M = Sm, Y)

	M = Sm	M = Y	
	Bond Distances (Å)		
M(1)−Ni(1)	3.0834(8)	3.0473(8)	4×
M(1)−Si(1)	3.101(2)	3.079(2)	2×
M(1)−Si(2)	3.006(1)	2.9752(9)	4×
	3.137(2)	3.102(1)	2×
M(1)−Si(3)	3.114(2)	3.087(2)	2×
Ni(1)−Si(1)	2.303(1)	2.286(1)	2×
Ni(1)−Si(2)	2.295(3)	2.262(2)	
Ni(1) −Si(3)	2.283(2)	2.272(1)	2×
Si(1)−Si(1)	2.344(5)	2.346(4)	
Si(1)−Si(3)	2.8186(7)	2.7893(8)	4×
Si(2)−Si(2)	2.409(3)	2.385(2)	2×
Si(3)−Si(3)	2.348(6)	2.350(4)	
	Bond Angles (deg)		
Ni(1)−M(1)−Ni(1)	80.02(3)	80.30(3)	2×
	81.06(3)	81.04(3)	2×
	132.16(4)	132.51(4)	2×
Si(1)−M(1)−Si(1)	79.47(6)	79.31(5)	
Si(1)−M(1)−Si(2)	81.12(5)	81.17(3)	4×
	126.29 (2)	126.35(2)	4×
	133.53(4)	133.57(3)	4×
Si(1)−M(1)−Si(3)	53.94(3)	53.79(2)	4×
Si(2)−M(1)−Si(2)	46.13(5)	46.18(5)	4×
	79.37(7)	79.32(7)	
	82.52(4)	82.66(4)	2×
	83.61(4)	83.43(3)	2×
	99.11(6)	99.04(6)	4×
	139.33(9)	139.28(6)	2×
Si(2)−M(1)−Si(3)	179.63(6)	179.78(6)	2×
	80.62(4)	80.80(3)	4×
	100.25(4)	100.45(4)	2×
	134.02(4)	133.93(3)	4×
Si(3)−M(1)−Si(3)	80.11(7)	79.78(5)	
Si(1)−Ni(1)−Si(1)	121.0(1)	119.98(9)	
Si(1)−Ni(1)−Si(2)	119.52(6)	120.01(4)	2×
Si(1)−Ni(1)−Si(3)	75.85(5)	75.45(3)	4×
Si(2)−Ni(1)−Si(3)	119.75(8)	120.15(5)	2×
Si(3)−Ni(1)−Si(3)	120.5(2)	119.69(9)	
M(1)−Si(1)−M(1)	79.47(6)	79.30(5)	
M(1)−Si(1)−Ni(1)	67.73(5)	67.35(4)	4×
Ni(1)−Si(1)−Ni(1)	121.0(1)	119.98(9)	
M(1)−Si(2)−Ni(1)	69.67(4)	69.64(3)	4×
	140.30(3)	140.33(2)	2×
M(1)−Si(3)−M(1)	80.11(7)	79.78(5)	
M(1)−Si(3)−Ni(1)	67.68(7)	67.33(4)	4×
M(1)−Si(3)−Si(1)	62.81(5)	62.96(4)	4×
	117.26(9)	117.12(5)	4×
Ni(1)−Si(3)−Ni(1)	120.5(2)	119.70(9)	
Ni(1)−Si(3)−Si(1)	52.39(4)	52.50(3)	4×
	127.66(8)	127.55(5)	4×
Si(1)−Si(1)−Si(3)	90.04(8)	90.04(5)	4×
Si(3)−Si(1)−Si(3)	89.39(3)	89.56(3)	2×
	90.61(3)	90.44(3)	2×
	179.9(1)	179.91(8)	2×
Si(1)−Si(3)−Si(1)	89.39(3)	89.56(3)	2×
	90.61(3)	90.44(3)	2×
	179.9(1)	179.91(8)	2×
Si(1)−Si(3)−Si(3)	89.96(8)	89.96(5)	4×
Si(2)−Si(2)−Si(2)	110.7(2)	110.9(1)	

Electronic Structure

An interesting issue here is how the valence electrons are distributed in these compounds. The assumption that the formal charge of Y and Sm would be 3+ is reasonable, because they are the least electronegative atoms in $SmNiSi_3$. This is also supported experimentally by the magnetic susceptibility measurements which are

consistent with Sm^{3+} centers and the absence of any measurable moment on Ni. Therefore, we can assign the electron distribution as $M^{3+}[NiSi_3]^{3-}$. Ni, however, is equally as electronegative as Si, and it is likely that Ni will neither accept nor donate electrons to Si. This makes $SmNiSi_3$ and $YNiSi_3$ essentially different from the typical Zintl type compounds. Simply on the basis of the electronegativity arguments, the formal charge on Ni might be expected to be either 0 or even negative. This will result in an electron-rich d^{10} configuration for Ni, which could be responsible for the relatively short Sm−Ni and Y−Ni distances of 3.0834(8) Å and 3.0473(8) Å, respectively. The Y−Ni distances are similar to those observed in YNiSi,[25] which range between 2.881 and 3.151 Å. The short distances may imply a certain amount of $Ni^0 \rightarrow Y^{3+}$ (and $Ni^0 \rightarrow Sm^{3+}$) dative bonding interactions.

To further address the electronic structure of these compounds, we performed electronic band structure calculations using both ab initio density functional theory (DFT) as well as the extended Hückel tight binding (EHT) approximation. The self-consistent electronic structure of $YNiSi_3$ was calculated within DFT using the full potential LAPW (linearized augmented plane wave) method implemented in WIEN97 code.[26] Both a scalar relativistic correction and spin−orbit interaction were included, although for these light atoms we do not expect relativistic effects to be significant. For the exchange and correlation parts of the potential we used the Perdew−Burke−Ernzerhof[27] potential, which incorporates a generalized gradient approximation (GGA). Self-consistency was carried out on a 36-point mesh in the irreducible monoclinic Brillouin zone.

The band structure is given in Figure 4, while the monoclinic Brillouin zone is shown in Figure 5 and the total and partial density of states (DOS) in Figure 6. It is clear that $YNiSi_3$ is a metal or a semimetal. The density of states at the Fermi energy is about 2.7 states/eV per unit cell (containing two Y, two Ni, and six Si atoms). An analysis of the partial density of states shows that all three types of atoms contribute roughly equally to the density of states at the Fermi energy. In addition, there is a large contribution in the DOS at the Fermi level from the nearly free electron interstitial charge distribution. On a broader scale, the bands lying in the range of 3 eV below the Fermi energy are primarily hybridized Ni d and Si p bands. The Si s band, predominantly coming from Si(2) (zigzag chain), lies below the hybridized d−p Ni/Si bands. The DOS above the Fermi energy are predominantly of Y d character, consistent with a Y^{3+} formal charge on this atom. There is, however, a small contribution of Y d orbitals in bands lying below the Fermi level, which originate from a certain degree of back charge transfer from the Ni or Si atoms. Although our LAPW method does not give appreciable Ni 4s character, the latter appears as nearly

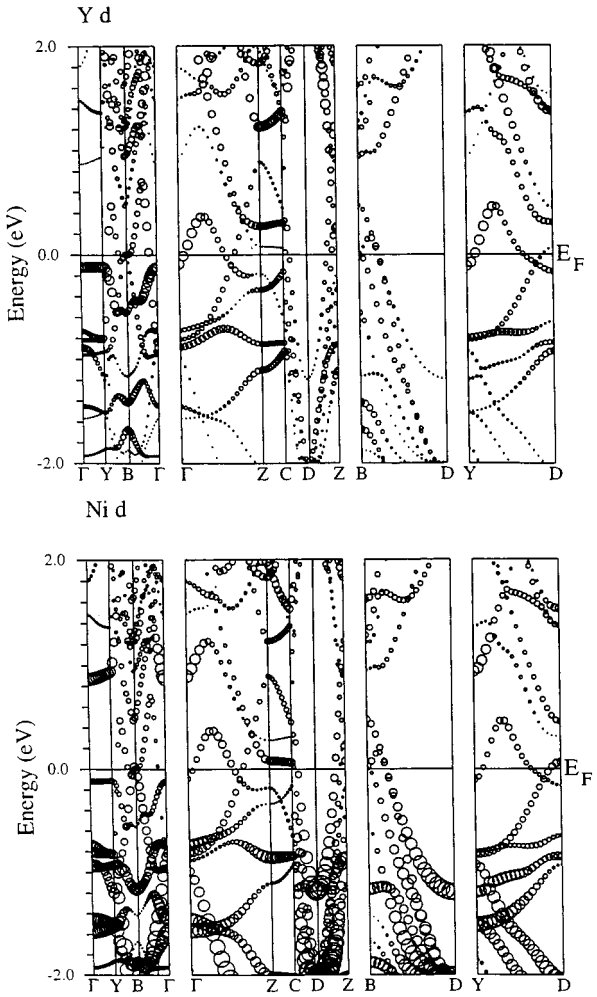

Figure 4. Electronic band structure for $YNiSi_3$ obtained from DFT−LAPW calculations with spin−orbit coupling included. The Fermi level has been arbitrarily set to zero. Orbital character plots of bands for $YNiSi_3$ obtained from DFT−LAPW calculations with spin−orbit coupling included. The size of the circle shown overlying the band structure plot is proportional to the orbital character at that point. The two largest contributions near the Fermi level, (A) Ni d and (B) Y d, are shown. The Fermi level has been arbitrarily set to zero.

free electron charge distribution in the regions between LAPW spheres. These charges can be assigned to either Ni or Si atoms. In our tight-binding calculation (see below) they appear as electrons in the Ni 4s orbital, making the Ni atoms reduced species. The calculated DOS rule out any oxidation on Ni (e.g. 2+ or 1+) and clearly suggest that the Ni d orbitals are filled, consistent with a Ni^0 d^{10} or even Ni^{2-} $d^{10}s^2$ configuration.

Since the transport properties of the compound are affected by the type and nature of the band(s) crossing the Fermi energy, we show the orbital character of these bands in Figure 4. The bands of interest are primarily hybridized Ni d and Y d bands. The degrees of Ni d and Y d character, however, are strongly k-dependent. A possible source of the small peak in the DOS near the Fermi energy could be the small dispersion of bands along the ΓY and CZ directions; see Figure 5. The Fermi surface of this material is rather complicated, with a small electronic pocket near the Γ point, hole-like pockets near the Y point, and both electron- and hole-like pockets straddling the Z point. The hole-like regions

(25) Hovestreydt, E.; Engel, N.; Klepp, K.; Chabot, B.; Parthe, E. *J. Less Common Met.* **1982**, *85*, 247−274.
(26) Blaha, P.; Schwarz, K.; Luitz, J. WIEN97: A Full Potential Linearized Augmented Plane Wave Package for Calculating Crystal Properties, Vienna University of Technology, Getreidemarkt 9/158, A-1060 Vienna, Austria.
(27) Perdew, J. P.; Burke, S.; Ernzerhof, M. *Phys Rev Lett* **1996**, *77*, 3865.

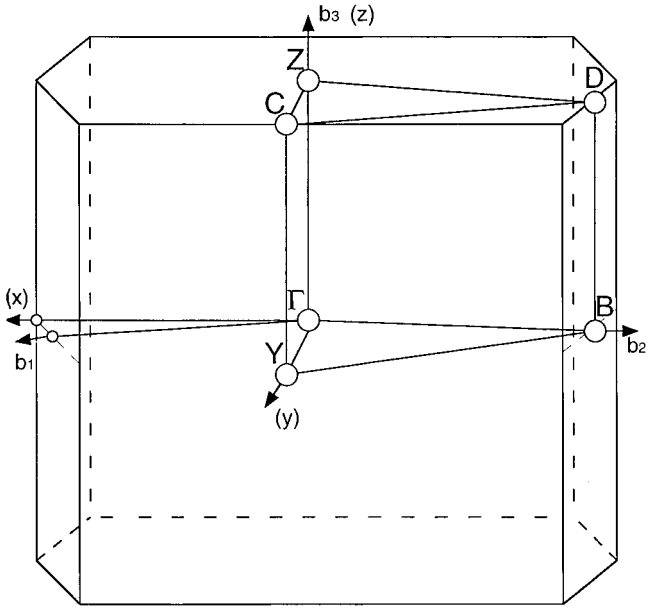

Figure 5. Monoclinic Brillouin zone associated with the band structure shown in Figure 4.

dominate the Fermi surface making the material a p-type metallic conductor (see below).

Additional insight into the bonding within the $NiSi_3$ framework, which is not readily obtainable from the DFT calculations described above, was gleaned from EHT calculations on the $[NiSi_3]^{3-}$ part of the structure.[28,29] Assuming that the formal charge of yttrium is 3+ in the compound, which is in agreement with the DFT band calculations, the yttrium atoms were not considered in the calculations. This calculation used an effective Hamiltonian of the EHT type,[30] and the parameters and exponents of Ni and Si atoms[31] were taken from previously published calculations.

Before examining the crystal orbital overlap population (COOP), one can attempt to assign formal charges to the network elements. The calculated charge distribution in the lattice suggests that the nickel atom has a negative formal charge of −2.5 (electron density = 12.51), while the Si(1) and Si(3) forming the dimers possess a slight positive formal charge of +0.2 (electron densities = 3.83 and 3.84, respectively). This is consistent with the coordination number (5) of these Si atoms and with the relatively close side-by-side approach between dimers (distance ∼ 2.8 Å). Therefore Si(1) and Si(3) seem to be slightly oxidized or neutral. On the contrary, the Si atoms forming the zigzag chain, Si(2),

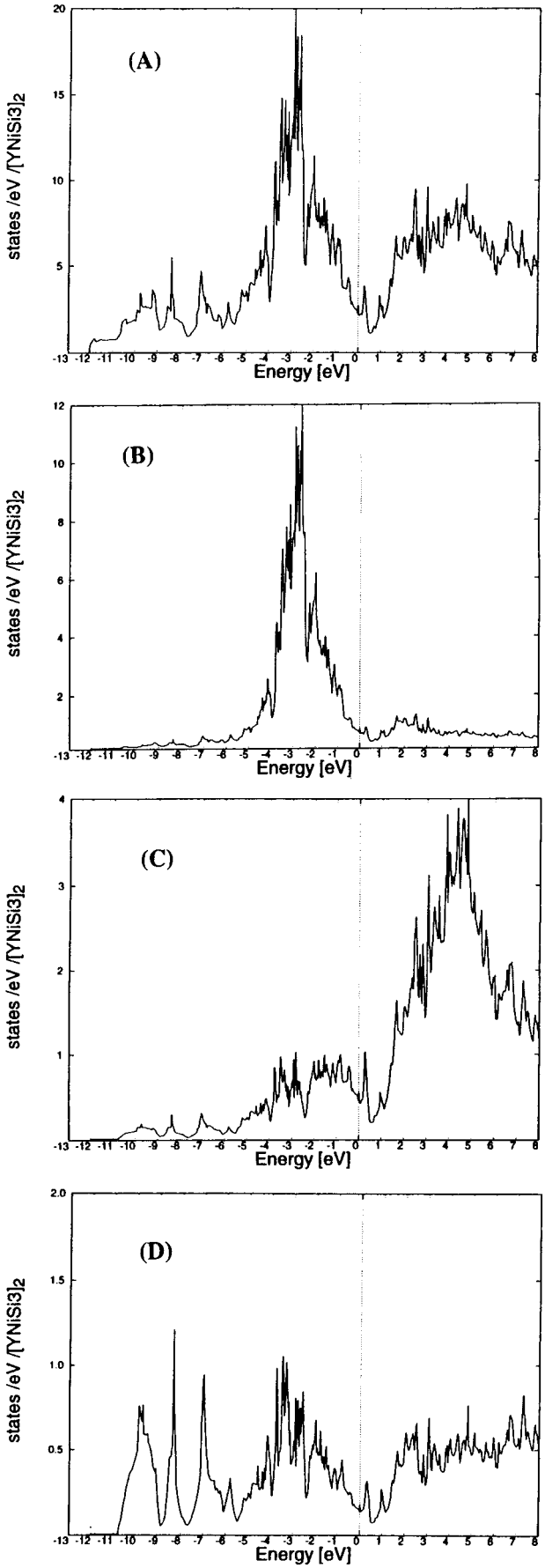

Figure 6. (A) One-electron total density of states for $YNiSi_3$. (B) Partial density of states including Ni d and s orbitals only. (C) Partial density of states including Y s, p, and d orbitals only. (D) Partial density of states including Si s and p orbitals.

(28) (a) Whangbo, M.-H.; Evain, M.; Hoffmann, R. EHMACC, program for Extended Hüchel Molecular and Crystal Calculations, North Carolina, **1987**. (b) Whangbo, M.-H.; Hoffmann, R. *J. Am. Chem. Soc.* **1978**, *100*, 6093−6098. (c) Hoffmann, R. *J. Chem. Phys.* **1963**, *39*, 1397−1412.

(29) The DFT−LAPW calculation was used to support our assumption that Y is best described as Y^{3+} and to justify our EHT calculation on the charged fragment $[NiSi_3]^{3-}$.

(30) The modified Wolfsberg−Helmholz formula is used to calculate the nondiagonal H_{ij} matrix elements: Ammeter, J.; Bürgi, H.-B.; Thibeault, J.; Hoffmann, R. *J. Am. Chem. Soc.* **1978**, *100*, 3686−3692.

(31) The atomic orbital parameters of Ni and Si are as follows: Ni: 4s = −10.95 eV (ζ_1 = 2.10), 4p = −6.27 eV (ζ_1 = 2.10), 3d = −14.20 eV (ζ_1 = 5.75, C_1 = 0.5683; ζ_2 = 2.30, C_2 = 0.6292); Si: 3s = −17.30 eV (ζ_1 = 1.383), 3p = −9.20 eV (ζ_1 = 1.383). (a) Summerville, R. H.; Hoffmann, R. *J. Am. Chem. Soc.* **1976**, *98*, 7240−7254. (b) Lauher, J. W.; Elian, M.; Summerville, R. H.; Hoffmann, R. *J. Am. Chem. Soc.* **1976**, *98*, 3219−3224. (c) Trong Anh, N.; Elian, M.; Hoffmann, R. *J. Am. Chem. Soc.* **1978**, *100*, 110−116.

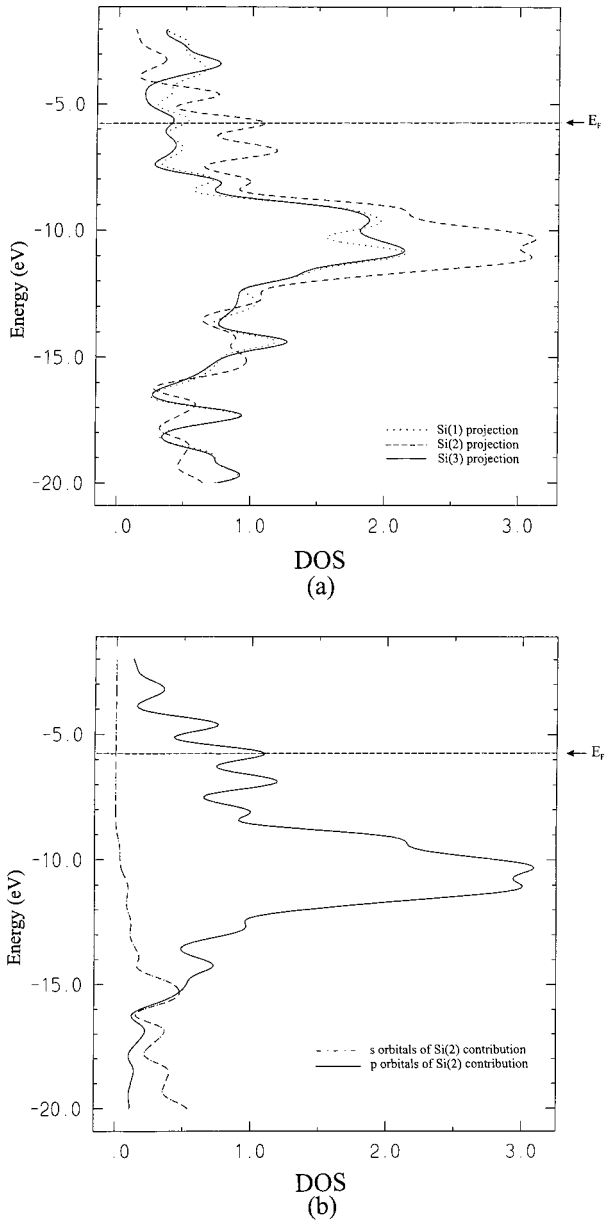

Figure 7. DOS diagrams for the $[NiSi_3]^{3-}$ framework obtained from EHT-tight binding calculations: (a) partial density of states corresponding to Si(1), Si(2), Si(3) projections and (b) partial density of states corresponding to s and p orbitals of Si(2) contributions. The Fermi level, marked with a dashed line, is drawn for the 100 electrons contained in the repeat unit made of 16 atoms (4 Ni and 12 Si).

are best thought of as reduced with a nearly −1 (actually −0.8) formal charge. While we do not place much emphasis on the calculated numbers, qualitatively the distribution of electron density seems plausible. The calculated negative formal charge on Ni and Si(2) atoms derives from the depletion of the electrons on Y atoms, which lie very close, with distances of Y−Ni ∼ 3.04 Å and Y−Si(2) ∼ 2.97 Å. The Pauling electronegativities for Ni (1.91) and Si (1.90) are very similar, which supports the formal charge assignment and the electron transfer.

The partial DOS diagram, corresponding to the contributions of the s and p orbitals of Si(2) (atoms in the zigzag chain), in Figure 7, shows that only the p orbitals of the silicon atoms are involved in the region near the Fermi level. Another interesting point is that

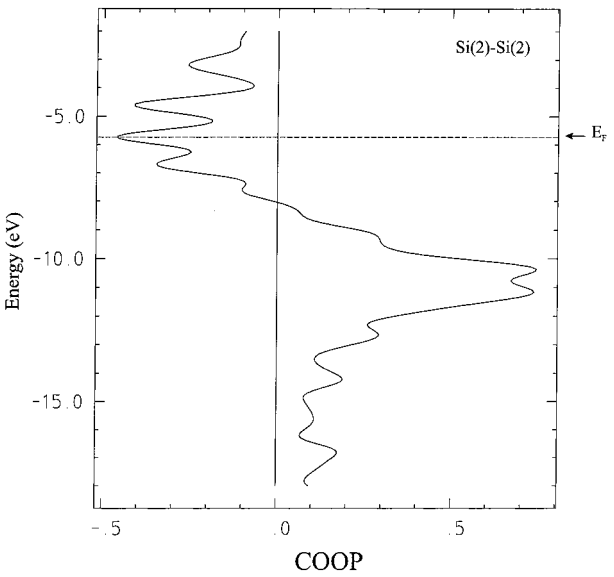

Figure 8. Crystal orbital overlap population (COOP) curve associated with the Si(2)−Si(2) bonds in the $[NiSi_3]^{3-}$ network. The Fermi level is shown as a dashed line for 100 electrons.

the Fermi level lies in a local DOS maximum only for the Si(2) atoms of the zigzag chain, which is associated with a π antibonding feature based on p_z orbitals. Below the Fermi level the π antibonding character persists until −8.0 eV and the π bonding interactions are localized between −9.0 eV and −8.0 eV; see the COOP curves in Figure 8. The π bonding levels are fully occupied and the π antibonding band is half-filled, consequently, according to the bond order rule, Si(2)−Si(2) possess a bond order of more than 1 and less than 2, corresponding to a full σ bond and partial π bond. Therefore, the zigzag chain of silicon atoms is much like that found in polyacetylene, only more reduced. Recently, a zigzag chain of Ge atoms in $LaNiGe_2$ was analyzed by the same computation method used here and was found to be very similar.[32]

The three different types of Si atoms in $[NiSi_3]^{3-}$ (labeled Si(1), Si(2), Si(3); see Figure 2), lead to four types of Si−Si bonds, as seen above, and therefore it would be interesting to examine the similarities and differences between each kind of Si−Si bond. The calculated overlap populations are as follows: 0.8729 for the Si(2)−Si(2) bonds (distance 2.385 Å), 0.8526 for Si(1)−Si(1) (distance 2.346 Å), 0.8377 for Si(3)−Si(3) (distance 2.350 Å), and 0.3116 for Si(1)−Si(3) (side-by-side distance of 2.8 Å). Despite the fact that the Si(2)−Si(2) bond is slightly longer than Si(1)−Si(1) and Si(3)−Si(3), it is suggested to be the strongest one. This observation is surprising, because a reasonable assumption would be to calculate the shortest bond as the strongest and most stable. Therefore, to understand this feature we have to consider the orbital contributions of the corresponding bands. One can explain the stronger Si(2)−Si(2) bond using the partial density of states associated with the s and p contributions from each of the three types of silicon atoms (Figure 7). The p character for the Si(2) is about two times larger than the p character for the Si(1) and Si(3) atoms. This last fact is also in good agreement with the presence of a σ

(32) Proserpio, D. M.; Chacon, G.; Zheng, C. *Chem. Mater.* **1998**, *10*, 1286−1290.

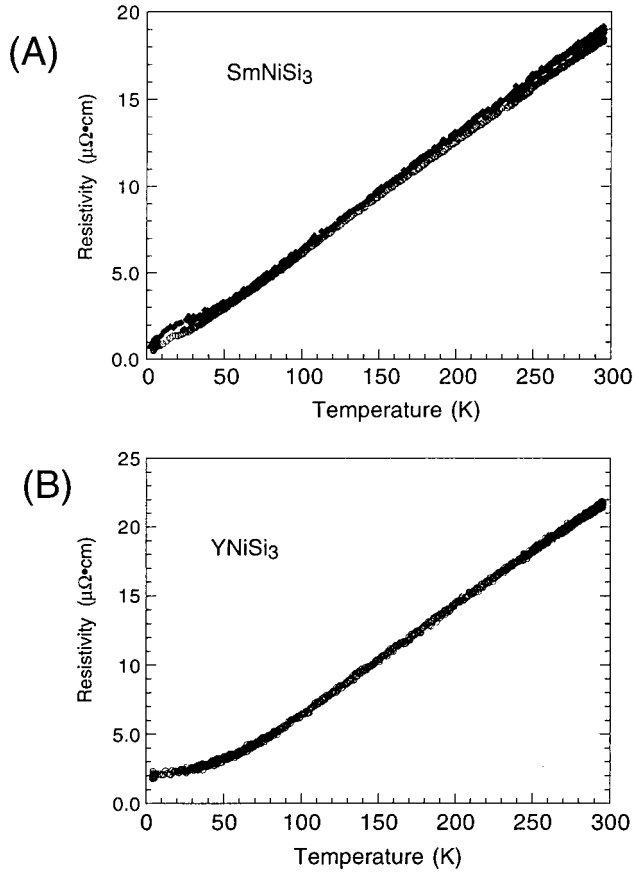

Figure 9. Variable temperature single-crystal electrical conductivity data for $MNiSi_3$ (M = Sm, Y).

bond as well as a weak double bond in the zigzag chain. At the Fermi level, the p orbital contribution for the chain is pointed in the direction of the yttrium orbitals, in accord with electron transfer from Y to Si(2). For the Ni atoms such an electron transfer is also implied by our calculations involving mainly Ni orbitals of s and p character.

Charge Transport and Magnetism

In agreement with the electronic band structure calculations, the electrical conductivity and thermopower data on single crystals of both compounds indicate metallic behavior. The room-temperature resistivity is very low in the range of 20−25 $\mu\Omega$ cm and decreases linearly with falling temperature, typical of metallic systems; see Figure 9. The Seebeck coefficient for both compounds was measured as a function of temperature and was found to be small (<10 μV/K) and positive throughout the temperature range studied; see Figure 10. The Seebeck coefficient is trending toward zero at 0 K. Therefore, we are dealing with metallic conductors in which the hole carriers dominate.

Magnetic susceptibility data for $SmNiSi_3$ are presented in Figure 11. The compound shows an antiferromagnetic transition at T_N = 12 K. Above 12 K, the magnetic susceptibility of $SmNiSi_3$ follows the modified Curie−Weiss law with $\chi_m = C/(T - \theta) + TIP_{Pauli}$, where TIP_{Pauli} is the temperature independent Pauli paramagnetism. The resulting Curie constant C is 0.0614 and the Curie temperature θ = −9.2 K. The estimated TIP_{Pauli} contribution is 7×10^{-4} emu/mol.[33] The effective

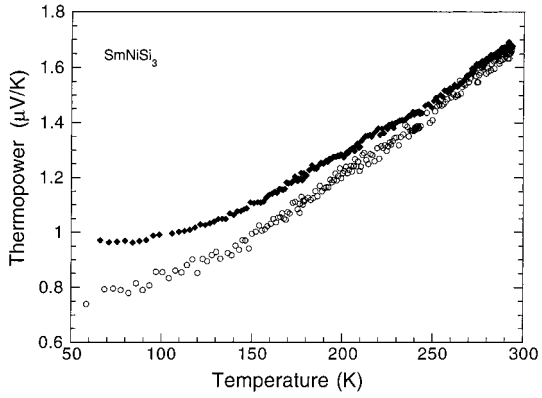

Figure 10. Variable temperature single crystal thermopower data for $SmNiSi_3$.

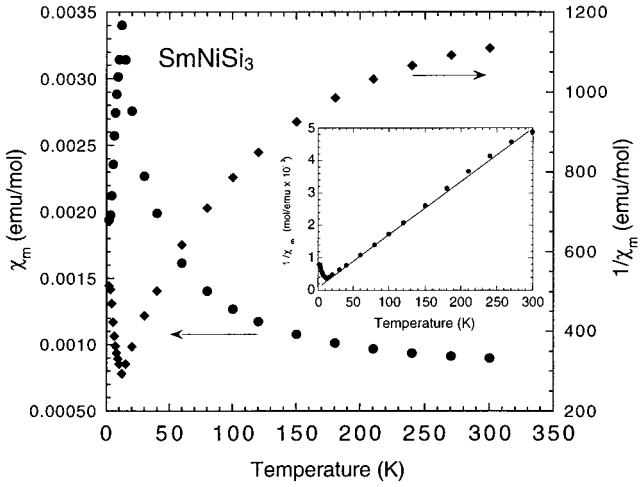

Figure 11. Plots of molar magnetic susceptibility (χ_m, emu/mol) and $1/\chi_m$ (mol/emu) vs temperature (K) for $SmNiSi_3$. The data were corrected for diamagnetic core contribution.

magnetic moment (μ_{eff}) at 300 K is 0.70 μ_B for $SmNiSi_3$, which is close to the theoretical μ_{eff} for Sm^{3+} (0.85 μ_B). There is no magnetic moment on the nickel atom, as it has also been found in many $RNiT_2$ compounds (R = rare earth metal, T = Si, Ge) which were studied by neutron diffraction. In $SmNiSi_2$,[22] μ_{eff} is 0.88 μ_B and Ni was found to have no magnetic contribution. It is interesting that $SmNiSi_2$ also has an antiferromagnetic transition with T_N = 9.8 K. The similar magnetic behavior between $SmNiSi_3$ and $SmNiSi_2$ can be understood on the basis of their similar structural features. In fact, the Sm atoms have the same coordination environment in both compounds. A detailed discussion about the magnetic ordering due to Sm−Sm interactions at low temperature can be found in ref 24. Magnetic susceptibility measurements on $YNiSi_3$ show only Pauli paramagnetism (~9×10^{-4} emu/mol), as expected for a metallic compound, with a very small amount of paramagnetic impurities becoming evident at low (<40 K) temperatures. With the theoretically calculated DOS (DFT theory), the Pauli susceptibility is found to be 5.5 $\times 10^{-4}$ emu/mol, in reasonable agreement with experiment. The observed Pauli paramagnetism is due to the conduction electrons in $YNiSi_3$ and it is also in accord with the absence of a moment for Ni, as would be expected for a system of d^{10} or a $d^{10}s^2$ configuration.

(33) The value has not been corrected for core diamangetism.

Concluding Remarks

Molten Ga is an excellent solvent for the synthesis and crystallization of the two new metallic ternary silicides $MNiSi_3$ (M = Sm, Y). We suggest the use of Ga as a promising synthetic method for synthesizing and crystallizing metal silicides and other tetrelides and at significantly lower temperatures than those required by conventional methods. The compounds $MNiSi_3$ (M = Sm, Y) crystallize in the $SmNiGe_3$ structure type, contain reduced Ni atoms, and do not obey Zintl's concept. The infinite zigzag Si chains are much like those in polyacetylene, but with some electron density in their π^* levels. The predominant charge carriers in these materials are holes. The new silicide $SmNiSi_3$ shows an antiferromagnetic transition at 12 K. The magnetic susceptibility data and the band structure calculations suggest that the oxidation state of Sm and Y is 3+ while that of Ni is 0 or −2.

Acknowledgment. M.G.K. is Camille and Henry Dreyfus Teacher Scholar 1993−1998. This work made use of the SEM facilities of the Center for Electron Optics at Michigan State University and the facilities of the Materials Research Center at Northwestern University (DMR-96-32472). We thank B. Sieve and M. Zhuravleva for help with the preparation of the manuscript.

Supporting Information Available: Tables of crystal data and structure refinement, anisotropic thermal parameters, and bond distances and angles for $MNiSi_3$ (M = Sm, Y) (12 pages); observed and calculated structure factors (4 pages). Ordering information is given on any current masthead page.

CM980447V